CHARACTERIZATION OF THE ROD-PINCH DIODE X-RAY SOURCE ON CYGNUS

B.V. Oliver[1], M. Berninger[3], G. Cooperstein[4], S. Cordova[1], D. Crain[3], D. Droemer[3],T. Haines[2], D. Hinshelwood[4], N. King[2], S. Lutz[3], C.L. Miller[5], I. Molina[1], D. Mosher[4], D. Nelson[1], E. Ormond[1], S. Portillo[6], J. Smith[2], T. Webb[1], D.R. Welch[5], W. Wood[2] and D. Ziska[6]

[1]Sandia National Laboratories, Albuquerque, NM 87185, USA
[2]Los Alamos National Laboratories, Los Alamos, NM 87545, USA
[3]National Security Technologies, Las Vegas, NV 89193 , USA
[4]Naval Research Laboratory, Wash. DC 20375, USA
[5]Voss Scientific, LLC, Albuquerque, NM 87108, USA
[6]KTech Corp, Albuquerque, NM 87123, USA

Abstract

The rod-pinch diode[1] is a self-magnetically insulated electron beam diode that is capable of producing a very bright source of hard x-rays. As fielded on the Cygnus accelerator[2], the diode operates at an impedance of 50 Ohms and produces short pulse (~50 ns) bremsstrahlung radiation with a 2 MeV photon endpoint energy and dose of 4 rad measured at one meter, with an x-ray spot size ~ 1mm. The source can be used to image through ~ 40 g/cm^2 of material with spatial resolution of order 300 μm. Recently, a series of experiments on Cygnus have been conducted to better characterize the diode's operation and x-ray output. In particular, the x-ray spectral content, source spot-size, and shot-to-shot reproducibility have been diagnosed. The intent of these experiments is to enable improvements that may extend the diode's radiographic utility. An array of diagnostics have been utilized which include, end-on and side view x-ray pin hole imaging, time resolved and time integrated spot size measurements, step wedges, x-ray p-i-n diodes, and diode/MITL current measurements. High fidelity, PIC/Monte-Carlo simulations have also been conducted to help analyze the data. An overview of these experiments, simulations, and the conclusions from analysis is presented.

I. THE ROD PINCH DIODE ON CYGNUS

The rod-pinch diode[1] consists of a solid Tungsten rod protruding through a circular cathode. Electrons emitted from the cathode become magnetically insulated and flow to the tip of the anode rod. Upon stopping in the rod, the electrons produce Bremsstralung X-ray radiation. The X-ray dose produced is a function of the electron current and energy (voltage) and the spot size is determined by the rod diameter. The diode operating impedance is determined by electron magnetic insulation in the presence of ions[3] with the current well described by the critical current formulation[3,4]

$$I = \alpha I_{crit}$$
$$I_{crit} = 8.5\frac{\sqrt{\gamma^2 - 1}}{\ln(r_c / r_A)} \qquad (1)$$

where $\gamma = 1 + eV/mc^2$ is the electron relativistic factor and α is a multiplicative factor ≅ 2.3. For diode operation at 2.25 MeV, the diode current I≅42 kA and the diode impedance = 53 Ohms.

On the Cygnus accelerator, the diode is fielded in positive polarity, such that the anode rod is attached to the accelerator center conductor (see Figure 1). Cygnus[2] is a 3 cell Induction Voltage Adder which produces a 2.4 MeV peak forward going voltage and a time averaged diode voltage between ~ 1.8-2 MeV. For the experiments discussed here, the anode rod is 0.75 mm diameter, with a 5 mm taper to the tip (see Figure 2).

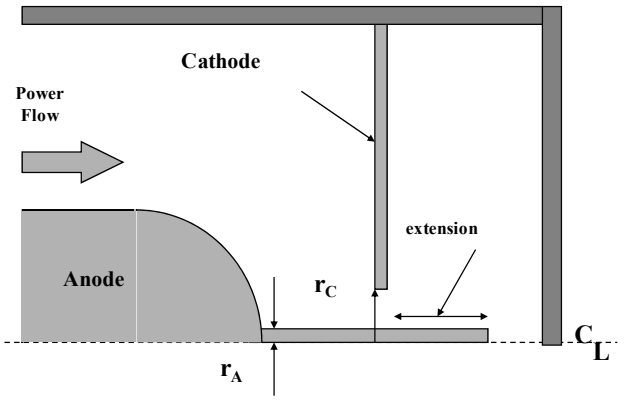

Figure 1. Illustration of the Rod Pinch diode.

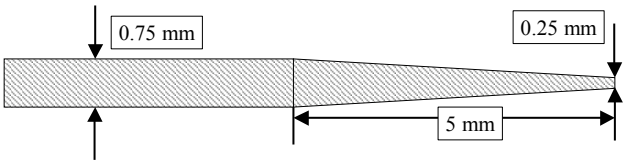

Figure 2. Illustration of the anode rod

Report Documentation Page

Form Approved
OMB No. 0704-0188

1. REPORT DATE	2. REPORT TYPE	3. DATES COVERED
JUN 2009	**N/A**	**-**

4. TITLE AND SUBTITLE	5a. CONTRACT NUMBER
Characterization Of The Rod-Pinch Diode X-Ray Source On Cygnus	5b. GRANT NUMBER
	5c. PROGRAM ELEMENT NUMBER
6. AUTHOR(S)	5d. PROJECT NUMBER
	5e. TASK NUMBER
	5f. WORK UNIT NUMBER
7. PERFORMING ORGANIZATION NAME(S) AND ADDRESS(ES) **Science Application International Corporation High Power Solutions Division Manassas, Va./Albuquerque, N.M.**	8. PERFORMING ORGANIZATION REPORT NUMBER
9. SPONSORING/MONITORING AGENCY NAME(S) AND ADDRESS(ES)	10. SPONSOR/MONITOR'S ACRONYM(S)
	11. SPONSOR/MONITOR'S REPORT NUMBER(S)

12. DISTRIBUTION/AVAILABILITY STATEMENT
Approved for public release, distribution unlimited

13. SUPPLEMENTARY NOTES
See also ADM002371. 2013 IEEE Pulsed Power Conference, Digest of Technical Papers 1976-2013, and Abstracts of the 2013 IEEE International Conference on Plasma Science. IEEE International Pulsed Power Conference (19th). Held in San Francisco, CA on 16-21 June 2013., The original document contains color images.

14. ABSTRACT
The rod-pinch diode[1] is a self-magnetically insulated electron beam diode that is capable of producing a very bright source of hard x-rays. As fielded on the Cygnus accelerator[2], the diode operates at an impedance of 50 Ohms and produces short pulse (~50 ns) bremsstrahlung radiation with a 2 MeV photon endpoint energy and dose of 4 rad measured at one meter, with an x-ray spot size ~ 1mm. The source can be used to image through ~ 40 g/cm2 of material with spatial resolution of order 300 Ým. Recently, a series of experiments on Cygnus have been conducted to better characterize the diode¡¦s operation and x-ray output. In particular, the x-ray spectral content, source spot-size, and shot-to-shot reproducibility have been diagnosed. The intent of these experiments is to enable improvements that may extend the diode¡¦s radiographic utility. An array of diagnostics have been utilized which include, end-on and side view x-ray pin hole imaging, time resolved and time integrated spot size measurements, step wedges, x-ray p-i-n diodes, and diode/MITL current measurements. High fidelity, PIC/Monte-Carlo simulations have also been conducted to help analyze the data. An overview of these experiments, simulations, and the conclusions from analysis is presented.

15. SUBJECT TERMS

16. SECURITY CLASSIFICATION OF:			17. LIMITATION OF ABSTRACT	18. NUMBER OF PAGES	19a. NAME OF RESPONSIBLE PERSON
a. REPORT	b. ABSTRACT	c. THIS PAGE			
unclassified	**unclassified**	**unclassified**	**SAR**	**6**	

An illustration of the Cygnus IVA cells, vacuum line, and diode region is shown in Figure 3a. A typical voltage profile is shown in Figure 3b).Voltage monitors fielded near the diode load (position 5) are generally unreliable for the duration of the radiation pulse (possibly due to bombardment by charged particles). Hence, voltage and current are measured upstream in the Cygnus vacuum line (position 3) and are transmission line shifted to obtain the voltage at the diode. The shifted voltage is in good agreement with position 5 measurements on shots where the position 5 monitor does not fail, as shown in Figure 3b).

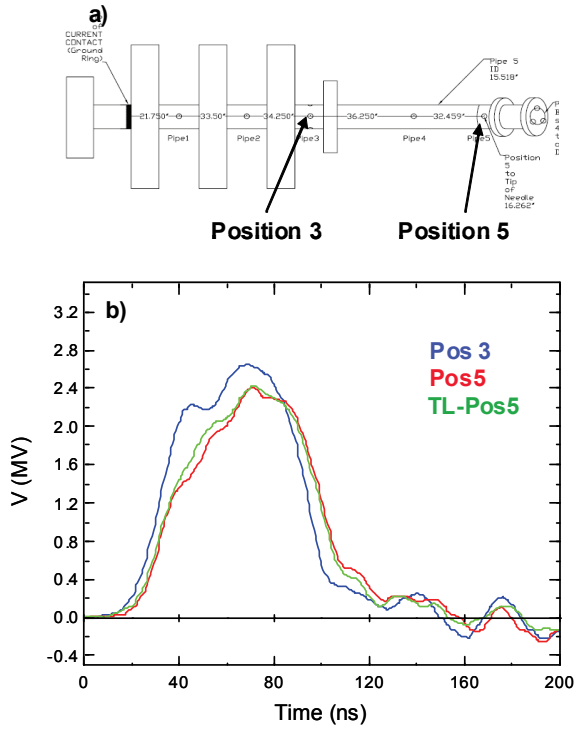

Figure 3. a) Illustration of the Cygnus IVA with the position 3 and 5 monitor locations. b) Measured voltage at pos. 3 (blue), pos. 5(red) and transmission line shifted voltage from pos. 3 (green).

Particle-in-Cell simulations coupled to Monte-Carlo transport calculations with the LSP code have characterized the radiation output from the rod-pinch[5] in terms of the current and voltage with dose-rate scaling as $dD/dt \propto IV^{1.25}$ (rads/ns), where D is the dose measured in rads at one meter, I is the diode current in amps and V is the diode voltage. Using the measured current and transmission line shifted voltage at the diode, the dose-rate scaling is in good agreement with the measured dose-rate, as demonstrated in Figure 4.

Over a sequence of shots, variations in voltage (both peak and average) as well as peak dose-rate are of order 10%. This results in an integrated dose output of 4.4 ±0.3 rads at one meter as shown in Figure 5.

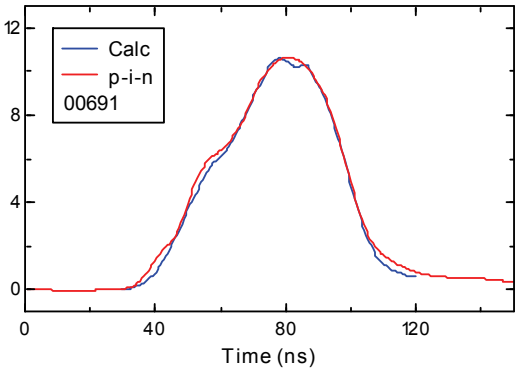

Figure 4. Calculated (blue) dose rate from current and voltage and measured (red) dose rate from p-i-n diodes.

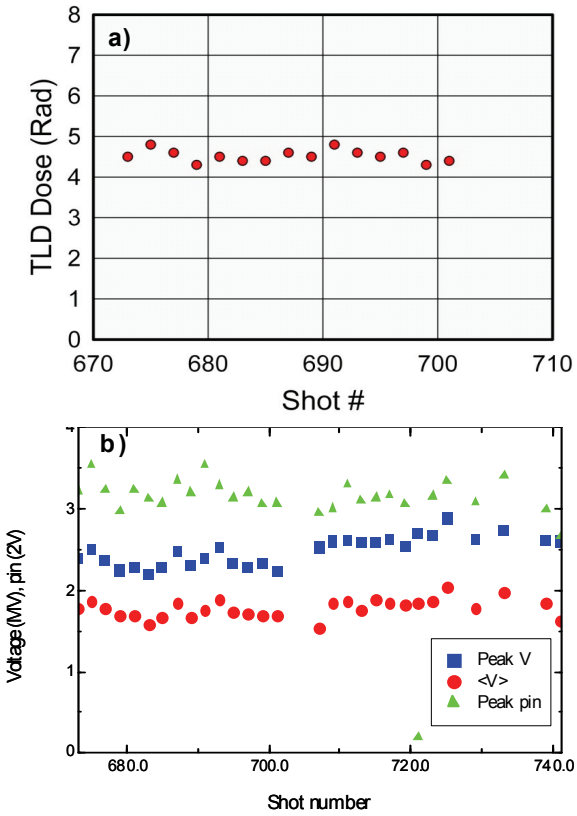

Figure 5. a) Dose vs. shot number on Cygnus 1 and b) peak voltage (blue), average voltage (red) and peak p-i-n signal (green) vs. shot number on Cygnus 1.

II. X-RAY IMAGING DIAGNOSTICS

A combination of both time resolved and time integrated x-ray diagnostics were fielded. 2-D rolled edges in conjunction with phosphor imaging plates were used to obtain side-on axial and radial source distributions as well as 2-D end-on distributions. The source spot size and distribution are obtained via measurement of the penumbral shadow region generated by the rolled edge

(see, for example, ref. [7]). In addition, the time-resolved-spot-size diagnostic (TRSD)[6] was fielded in both a side-on (axial) and an end-on configuration to gain information about the dynamic evolution of the source spot-size. A wide field of view x-ray pin-hole (1.2mm diameter) camera was also fielded in a side viewing geometry at 3.5° off normal (to the axis) at a demagnification of 0.45. The layout for the side viewing rolled-edge and pin-hole camera is shown in Figure 6. End on imaging also includes Ta step wedges and a 1 cm Ta rod, used for obtaining spectral information and mass density reconstruction.

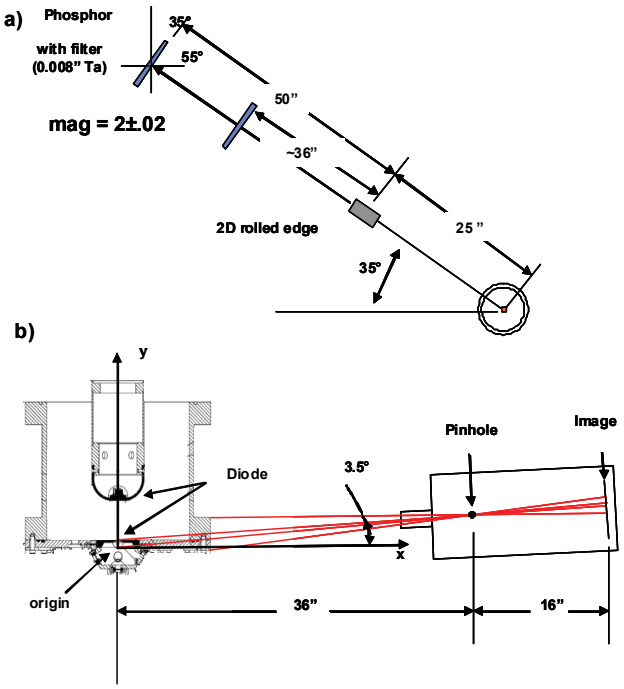

Figure 6. The side viewing diagnostic layout a) rolled-edge and b) pin-hole camera

III. X-RAY IMAGING RESULTS

Results from measurement of the end-on spot size are shown in Figure 7. The source edge-spread and line spread function are plotted, which result in an AWE definition [7] spot-size of 1.1mm. The full width half-maximum of the line-spread is 0.71mm and indicates a well defined core with little contribution from x-rays generated in the wings of the distribution.

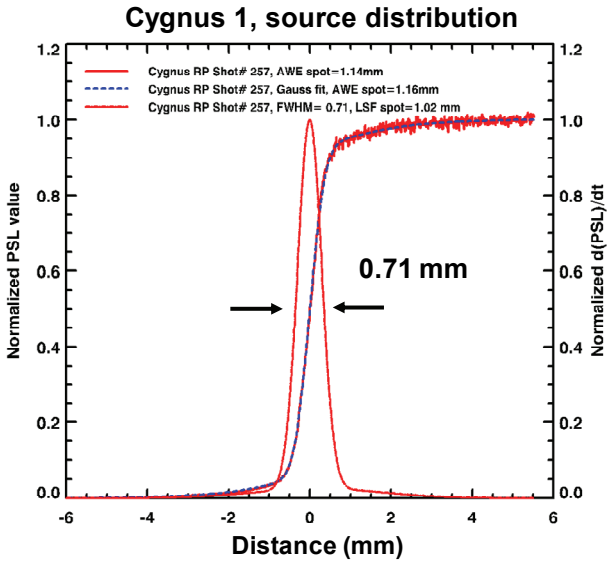

Figure 7. The edge-spread and line spread function from end-on imaging of the rod-pinch. The distribution results in a 1.1 mm spot-size

A typical pin-hole camera image is shown in Figure 8. The log-scale image of intensity (integrated over the pulse duration) indicates x-ray production from the rod tip, cathode plate, entire extent of the rod, and the base holder for the rod (which is located at the end of the Cygnus transmission line). The low intensity region (dark) seen in the region between the cathode plate and approximately half way upstream towards the base holder is due to increased mass within the line of sight. Analysis of the emission observed from the cathode plate suggests that it is primarily due to scattered photons emitted from the rod tip [8]. The down scattered photon spectrum is significantly softer than the main rod-tip emission and spans an approximately 2cm diameter. This extended source is not desired, however, due to its large area and low energy, it can be effectively collimated and removed from the downstream imaging line of sight.

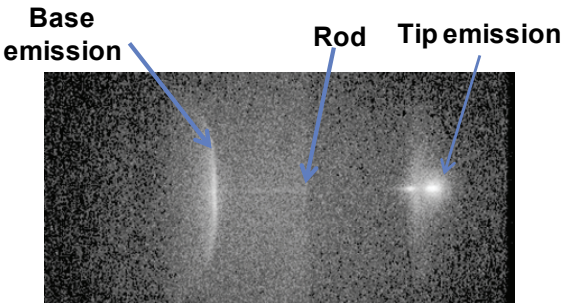

Figure 8. Side-viewing pin-hole image.

A more influential problem is the extended source observed in the rod base region. An X-ray coronagraph measurement is made to estimate the intensity of the extended source relative to the rod tip. A Pb plug is placed in the center of the image plane, near the rod tip to block the primary tip emission while allowing for unobstructed transmission of the base emission. The line spread function (LSF) is measured in a low magnification (1.2) downstream end-on geometry, and is shown in Figure 9. The measured asymmetry in the LSF is due to the angle of observation which is slightly off axis. Also shown is the calculated intensity assuming the Pb plug is removed. The calculated intensity assumes a double Gaussian distribution that matches the extended coronal region and models the source distribution with the assumption of no Pb attenuation. The Pb plug attenuates approximately 98% of the rod-tip emission. Comparison suggests that the base emission has an ~ 23mm diameter and accounts for upwards of 10% of the dose. Its large area, and thus low intensity, makes collimation of the majority of the source easy, however, emission at radii close to the rod cannot be removed from the end-on line of sight. The large dose contribution suggests that the radiation is most likely due to direct impact of electrons from the cathode to the base. Assuming the measurement is accurate, it implies that greater than 10% of the diode current is reaching this region, specifically because the base material has low atomic number (Stainless Steel) relative to the Tungsten rod and is thus a less efficient bremsstrahlung producer.

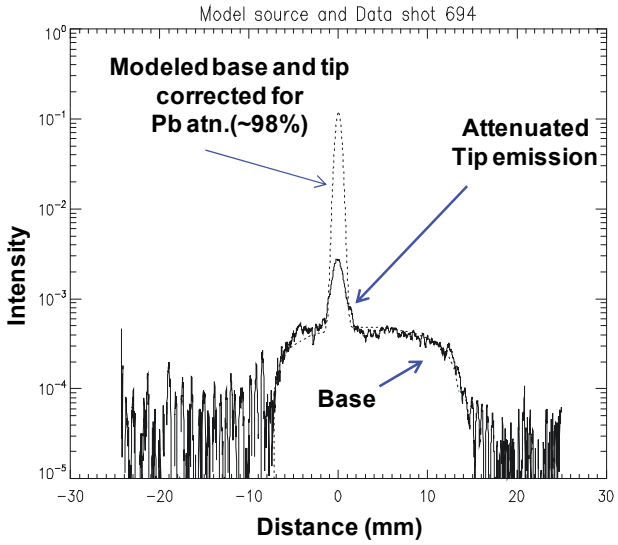

Figure 9. Log intensity vs. distance of the line-spread function from the X-ray coronograph: meausered data (solid) and calculated assuming Pb plug removed (dashed).

Results from end-on imaging of the time dependent spot size are shown in Figure 10. The measurement is made with the TRSD which streaks in time the penumbral region of the shadow cast by a 1-D rolled edge. The edge spread function (ESF) is measured and then the spot size determined. False color contours of the radiation intensity from the shadow image cast by the rolled edge (top half of image is exposed and bottom half is in the shadow) are shown. Vertical line-outs of the image result in ESF's. Both the AWE definition spot-size and movement relative to the time averaged centroid (peak of the distribution) are plotted vs. time. Spot growth occurs during the pulse growing from ~ 0.8 mm at the beginning to 1.4 mm by the end of the pulse. To within the uncertainty of the measurement (~ 0.25mm) no motion of the centroid is measured.

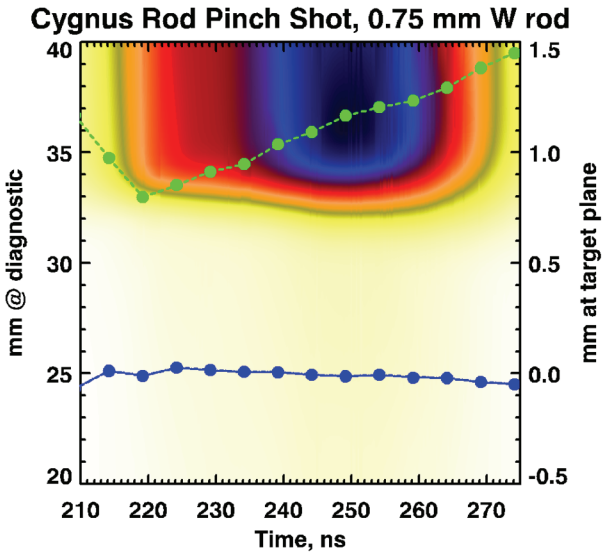

Figure 10. False color contours of the image intensity from the time dependent rolled edge measurement. Analysis of vertical lineouts of the image yield the end on spot size (green) and centroid position (blue) vs. time.

Side on imaging with the TRSD diagnostic demonstrates both growth in the axial extent of the source and movement from the rod tip towards the cathode (upstream). In Figure 11 the spot centroid position and axial spot size are plotted. The data demonstrates that the position begins near the anode tip and moves upstream approximately 2.3 mm during the pulse duration. The axial spot size varies from ~ 3 mm extent to 7 mm extent (and monotonically grows) throughout the pulse. Shot to shot variation in the time dependence of the axial distribution is observed, but has not yet been correlated with source performance.

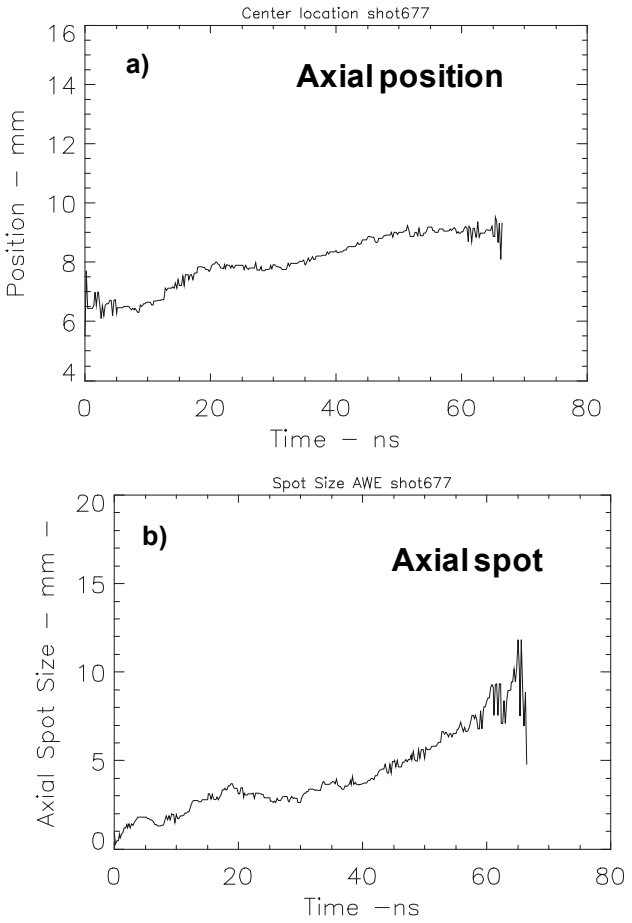

Figure 11. Time dependent side-on imaging. a) spot centroid position, b) spot size

IV. SPECTRAL MEASUREMENTS

Both simulation and measurement of the rod-pinch spectral distribution are reported. Particle-n-cell (PIC) coupled to Monte-Carlo electron and photon transport simulations are conducted with the LSP code[9] to characterize variation in the spectral content due to voltage fluctuations [10]. Because the rod is not range thin, electrons make multiple passes through the rod and thus produce a bremsstrahlung photon spectrum which is significantly softer than expected from a paraxial electron beam striking an optimized converter target. Simulations conducted with endpoint voltages of both 2.1 and 1.8 MV confirm that the total output dose scales as $IV^{1.25}$ indicating a 40% decrease in output for the lower voltage simulation (we note that the diode impedance is 53 Ohms and thus the current scales linearly with the voltage as I=53*V). However, the overall profile of the generated photon spectrum within a 15^0 cone about the axis is little changed except at the high energy end of the spectrum, as shown in Figure 12. Only the end point energy is substantially changed between the two simulations. It should be noted that these simulations have not included the effects of electrode plasmas, which we expect could influence the spectrum.

Similar conclusions are obtained from measurement of the transmission through a 1 cm diameter Ta rod. The spectrum is inferred by inverting the integral equation

$$d_i(x) = \int_{Energy} F_i(E) \times S(E,x) dE$$

where $d_i(x)$ is the transmission data, $F_i(E)$ is the energy dependent Filter/Detector response, and S(E,x) the spectrum. The calculations are in part constrained by specifying the minimum and maximum photon energy. The inferred spectrum for a series of 13 separate shots are shown in Figure 13 and demonstrate ~ 4% variation in profile in the energy range from 100keV – 1 MeV, and slightly larger variation (> 5%) in the high energy tail. The conclusions are supported by analysis of attenuation data which suggests a less than 4% variation in transmission through the Ta rod, shot to shot. In Figure 14 the % variation in transmission from a number of shots is plotted as a function areal mass. When viewing through low and high areal masses (< 5 g/cm^2 and > 30 g/cm^2, respectively) the variation is of order 4%, however, at the mid mass levels (between 5 and 30 g/cm^2) the variation is less and of order ~ 2%, implying that the mid energy photon spectrum is little changed shot to shot. Importantly, this variation is a factor 2.5 times smaller than the measured variation in the average and peak voltage of the Cygnus accelerator.

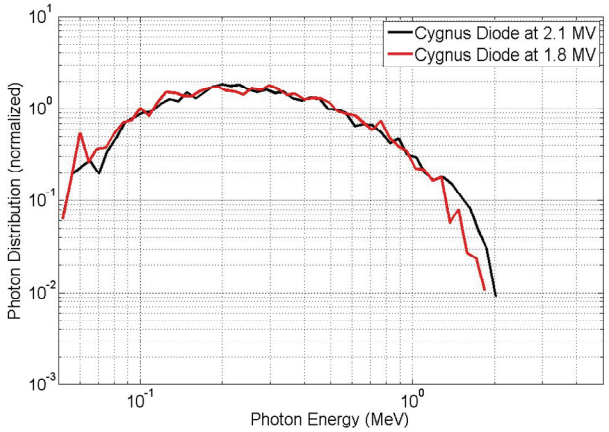

Figure 12. Comparison of the normalized (by the total dose) photon energy spectra for the 2.1 MV (black) and 1.8 MV (red) Cygnus diodes.

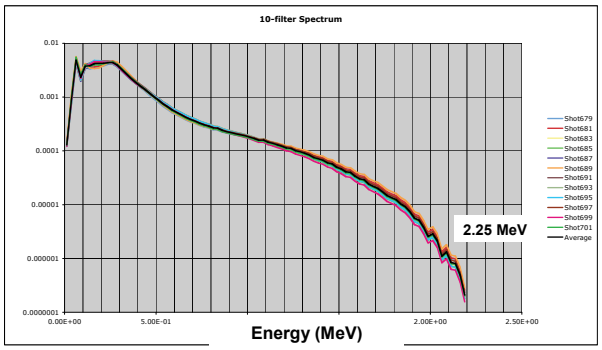

Figure 13. Photon spectrum for 13 seperate rod-pinch shots.

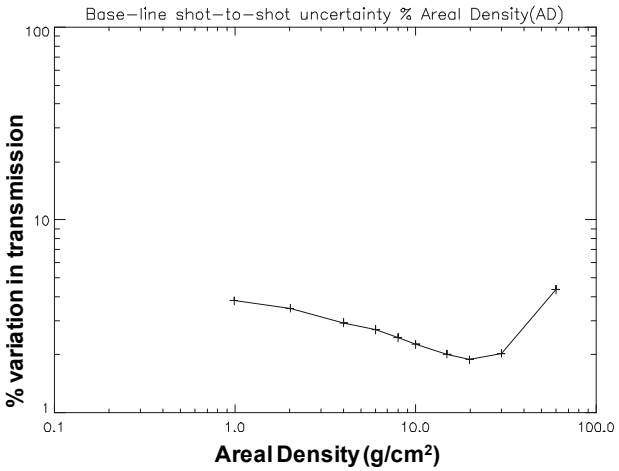

Figure 14. Variation in transmission as a function of areal density

VI. CONCLUSION

A study to characterize the rod-pinch diode as fielded on the Cygnus accelerators is reported. Voltage fluctuations and total dose output vary by ~ 10%, with the dose scaling as $IV^{1.25}$. A large diameter (~23 mm) extended source is identified at the base of the rod holder and may account for up to ~ 10% of the dose production. It is believed to have subtle radiographic influence due to its low intensity. It is concluded that X-rays observed emanating from the cathode are due to scattered x-rays originating from the source and are easily shielded from downstream diagnostics because of their low energy and large diameter. Time resolved measurement of the spot size, both end-on and along the rod tip, were made. Conclusions are that the end-on spot is dynamic and grows throughout the pulse at a rate of ~ 12μm/ns, with a time integrated value of 1.1 mm. In addition, the axial spot is dynamic, both growing in extent and moving from the rod-tip towards the base (upstream). The time integrated value of the axial spot-size is ~5-6 mm and variable from shot to shot. Total motion of the axial spot in the upstream direction is approximately 2.4 mm and variable.

PIC/Monte-Carlo simulations of the rod-pinch were conducted to generate synthetic spectrum. The studies conclude that the total dose and the high energy component (> 1.6 MeV) of the spectrum is most greatly affected by voltage fluctuations. However, the overall spectral profile in the forward direction (within a 15° cone) is little changed. This is supported by measurements where the spectral information is obtained by analyzing x-ray transmission through both Ta step-wedges and a solid Ta rod. It is determined that the time integrated spectral variations are dependent on energy but are less than 4% over the entire energy range from 40 keV to 2 MeV and variations are of order 2% at the 100keV-1 MeV range. Further it is determined that for areal mass densities in the 10-30 g/cm^2 range the variation in transmission shot to shot is ~2%.

VII. ACKNOWLEDGEMENTS

This work is funded by the U.S. Department of Energy through Sandia National Laboratories. Sandia is a multiprogram laboratory operated by Sandia Corporation, a Lockheed Martin Company, for the United States Department of Energy's National Nuclear Security Administration under contract DE-AC04-94AL85000.

VIII. REFERENCES

[1] R. A. Mahaffey, J. Golden, S. A. Goldstein, and G. Cooperstein, Appl. Phys. Lett. **33**, 795 (1978).
[2] D. Weidenheimer et al, Proc. 13th Pulsed Power conf. (2001); J.R. Smith et al., Proc. 14th Intl. Conf. on High Power Particle Beams (2002).
[3] B.V. Oliver, P.F. Ottinger, T.C. Genoni, et al. Phys. Plasmas, **11**, (2004);
[4] G. Cooperstein, J.R. boller, R.J. Commisso et al. Phys. Plasmas, **8**, 4618 (2001)
[5] D. V. Rose, D. R. Welch, B. V. Oliver, et al. J. Appl. Phys. **91**, 3328 (2002).
[6] S. Portillo, et al., IEEE Trans. Plasma Sci**. 34,** 1908**,** (2006)
[7] T. Goldsack, T.F. Bryant, P.F. Beech et al. IEEE Trans. Plasma Sci., **30**, 239 (2002)
[8] D. Mosher et al., these proceedings, paper O1-4.
[9] T. P. Hughes, S. S. Yu, and R. E. Clark, Phys. Rev. **2**, 11041 (1999).
[10] C.L. Miller and D.R. Welch, these proceedings, paper O1-3